

# Generalized Records for Functional Time Series with Application to Unit Root Tests

Israel Martínez-Hernández<sup>1</sup> and Marc G. Genton<sup>1</sup>

July 19, 2022

## Abstract

A generalization of the definition of records to functional data is proposed. The definition is based on ranking curves using a notion of functional depth. This approach allows us to study the curves of the number of records over time. We focus on functional time series and apply ideas from univariate time series to demonstrate the asymptotic distribution describing the number of records. A unit root test is proposed as an application of functional record theory. Through a Monte Carlo study, different scenarios of functional processes are simulated to evaluate the performance of the unit root test. The generalized record definition is applied on two different datasets: Annual mortality rates in France and daily curves of wind speed at Yanbu, Saudi Arabia. The record curves are identified and the underlying functional process is studied based on the number of record curves observed.

**Some key words:** Functional random walk; Functional unit root test;  $I(1)$  functional processes; Non-stationary functional time series; Functional depth.

**Short title:** Generalized Records for Functional Time Series

---

<sup>1</sup> Statistics Program, King Abdullah University of Science and Technology, Thuwal 23955-6900, Saudi Arabia.  
E-mail: israel.martinezhernandez@kaust.edu.sa, marc.genton@kaust.edu.sa  
This research was supported by the King Abdullah University of Science and Technology (KAUST).

# 1 Introduction

The record theory has been studied extensively for a sequence  $\{W_1, \dots, W_n\}$  of identically distributed univariate random variables for both independent and dependent data (Sparre Andersen, 1954; Feller, 1971; Ballerini and Resnick, 1987; Lindgren and Rootzén, 1987; Burridge and Guerre, 1996; Ahsanullah and Nevzorov, 2015). Record theory is part of the study of order statistics theory and extreme value theory. It studies the events that exceed all previous observations, i.e.,  $W_n > \max\{W_1, \dots, W_{n-1}\}$ , which are relevant to many phenomena, e.g., studying temperature records, studying high-temperature superconductors in physics, studying records in stock prices, and monitoring production. The two most studied quantities of records are the probability for a record at time  $n$  and the number of records observed up to time  $n$ . It is well known that the expected number of records for stationary time series grows at rate  $\log n$  (Lindgren and Rootzén, 1987). On the other hand, if the time series is a random walk process, the growth rate is  $n^{1/2}$  (Sparre Andersen, 1954; Feller, 1971; Burridge and Guerre, 1996). Moreover, if the time series has a linear trend component, then the number of records grows at rate  $n$  (Ballerini and Resnick, 1987). Extensions of the study of records to multivariate data can be found in the literature (see Goldie and Resnick, 1989, 1995; Gnedin, 1998). For multivariate data, different types of records have been defined, such as complete, simple or partial records, since there are more than one observation that can reach a new maximum (Wergen et al., 2012; Dombry and Zott, 2018; Falk et al., 2018).

Due to modern technologies, data can now be collected on a large scale and in an automatic fashion for many phenomena, resulting in high-dimensional and high-frequency data, that can be considered as continuous functions or surfaces (images). For example, in economy, finance, climatology, medicine, biology, and engineering, data can be collected with characteristics that vary along a continuum (time or space). Functional Data Analysis (FDA) deals with this type of data and has become an important research area in statistics (see, e.g., Ramsay and Silverman, 2005). Thus, record theory is as important in functional data as in univariate (multivariate)

data. However, much less is known about records in functional data. It is not natural to extend the multivariate approach to functional data, since a curve is considered as a single entity, and because of the infinite dimension of the space of continuous functions. Here, we propose a new concept of records for time series of functional data (functional time series) referred as *functional records* or *record curves*, and we study the behavior of the number of functional records.

One of the challenges for functional data (as well as for multivariate data) is that there is no natural way to define an order on this space. A paper by [Fraiman et al. \(2014\)](#) seems to be the first effort to extend the concept of records to functional data. They used the notion of records to define and detect deterministic trends in temperature curves. In that paper, a curve is said to be a record if the time at which the curve is a pointwise record is higher than the rest of the curves. Although this definition is useful, it cannot be applied to general cases, since it does not involve any ranking of curves or take into account the properties of the curves. The idea of using functional records to define deterministic trends is interesting, since the study of trends in an infinite-dimensional space is challenging and can easily be confused with stochastic trends, e.g., the functional autoregressive model in [Example 1](#) below. However, with the right definition of a functional record, one can obtain the same results as in univariate time series, i.e.,  $\log n$ ,  $n^{1/2}$ , and  $n$  as the growth rates of the number of functional records for stationary, stochastic trends, and deterministic trends components, respectively. That is, we can define and detect different tendencies by using the growth rates of the number of functional records. Here, we propose a general extension of the definition of records by using an order for functional data based on depth notions. Then, we study the behavior of the number of functional records (the two most extreme curves) under stationarity and under stochastic trend components. As an application of the functional records theory, we propose a unit root test in functional times series.

Several notions of depth (called functional depth) have been proposed for functional data, including integrated depth ([Fraiman and Muniz, 2001](#)), band depth and modified band depth ([López-Pintado and Romo, 2009](#)), half-region depth based on hypographs and epigraphs ([López-](#)

Pintado and Romo, 2011), spatial depth (Chakraborty and Chaudhuri, 2014b) and extremal depth (Narisetty and Nair, 2016). Other functional depth definitions can be found in Nieto-Reyes and Battey (2016), Gijbels and Nagy (2017), and Huang and Sun (2019). Depth has been used in different statistical problems. For example to detect outliers, to obtain robust estimators and to define functional boxplots, taking advantage of its center-outwards order (Rousseeuw and Hubert, 1999; Fraiman and Muniz, 2001; Sun and Genton, 2011; Sguera et al., 2014; Martínez-Hernández et al., 2019). The order induced by the functional depth can be viewed as order statistics. Unlike the usual order statistics in  $\mathbb{R}$ , ordered from the smallest value to the largest, the order based on depth starts with the most central curve that corresponds to the highest depth value, and moves further away from the center, ending with the most outlying curve that corresponds to the smallest depth value. We use this center-outwards ordering to define functional records.

In this paper, we are interested in studying two applications of functional time series: wind speed curves in Saudi Arabia and mortality rates in France. Let  $X_i(s)$  be the daily curves of wind speed at 80m [ $m/s$ ] where  $i = 1, \dots, n$  represents the day, and  $s \in [0, 24)$  represents hours within a day. The study of the wind speed curves is important for renewable energy generations. By using record curves, we can describe the dynamics of the record daily wind speed. It is relevant to know when and how often a record curve is observed to predict the efficiency of wind turbines and to prevent disruption and possible damage to a wind farm. A pointwise record may not provide enough information, unless it lasts more than one time point observation. Therefore, a univariate approach to detect records is not appropriate. Our approach identifies when a functional record is observed and provides information on the number of new functional records expected. Now, let  $X_i(s)$  denote the mortality rate in year  $i$ , at age  $s$ . It is important to know (besides prediction) how these rates behave over the years, taking into account all ages. By studying the functional records, we analyze whether the new functional records over the years correspond to the natural randomness of the process, or if there is an indication of a decreasing

trend. In general, the number of functional records provides information about the stationarity and nonstationarity properties of the functional time series.

The main contributions presented in this paper are: 1) the establishment of a generalized definition of upper and lower record for functional time series, and using the order induced by functional depth to rank curves to set a new record when there is a new minimum functional depth value; 2) the study of the growth rate of the number of functional records over time, under stationarity and nonstationarity assumptions; and 3) the introduction of a unit root test for a general integrated of order one ( $I(1)$ ) functional process, as an application of the functional record.

The remainder of our paper is organized as follows: In Section 2, we introduce mathematical concepts for functional data, functional time series, and functional depth. In Section 3, we describe an extension of records to functional data. In Section 4, we study the properties of the number of functional records, both for stationary and nonstationary functional time series. In Section 5, we propose a unit root test as an application of the study of functional records. In that section, we conduct a simulation study to evaluate the performance of the proposed test. In Section 6, we study the record curves on two different datasets: the daily curves of wind speed at Yanbu, Saudi Arabia, and the annual mortality rates for males in France. Section 7 presents some discussion. Proofs are provided in the Appendix. Additional material can be found in the Supplementary Material.

## 2 Preliminaries

### 2.1 Functional time series

Throughout this paper, we refer to a functional time series as  $X_i$  or  $X_i(s)$  without further clarification unless it is needed. Let  $(\Omega, \mathcal{F}, P)$  be a probability space,  $X$  be a random variable defined on a separable Hilbert space  $\mathcal{H}$ ,  $X : \Omega \rightarrow \mathcal{H}$ , where  $\mathcal{H}$  is a set of square integrable functions defined on a compact subset  $\mathcal{T} \subset \mathbb{R}$ , equipped with an inner product  $\langle \cdot, \cdot \rangle$  and a norm

$\|\cdot\|_{\mathcal{H}}$ . Without loss of generality, we assume  $\mathcal{T} = [0, 1]$ . Let  $L_{\mathcal{H}}^2 = \{X : \Omega \rightarrow \mathcal{H}; \mathbb{E}(\|X\|_{\mathcal{H}}^2) < \infty\}$  be the set of random variables  $X$  of  $\mathcal{H}$  with finite second moment. We define the norm in  $L_{\mathcal{H}}^2$  as  $\|X\|_{L_{\mathcal{H}}^2} = \{\mathbb{E}(\|X\|_{\mathcal{H}}^2)\}^{1/2}$ ,  $X \in L_{\mathcal{H}}^2$ . If  $X \in L_{\mathcal{H}}^2$ , then the expected value of  $X$ ,  $\mu$ , is defined as the unique element of  $\mathcal{H}$ , such that  $\mathbb{E}(\langle X, z \rangle) = \langle \mu, z \rangle$ , for all  $z \in \mathcal{H}$ . We denote by  $\mathcal{C}(\mathcal{H})$  the space of all probability measures on  $\mathcal{H}$ . If  $X$  is a functional random variable with distribution  $P \in \mathcal{C}(\mathcal{H})$ , we write  $X \sim P$ , and it is said to be symmetrically distributed ( $P$  is centrally symmetric) about  $z \in \mathcal{H}$  if and only if  $X - z = -(X - z)$  in distribution.

A functional time series is a sequence of random variables  $\{X_i, -\infty < i < \infty\}$  on  $\mathcal{H}$ . Assuming that  $\{X_i\} \in L_{\mathcal{H}}^2$ , the covariance operator at lag  $h$  is defined as  $C_{X_{i-h}, X_i}(z) = \mathbb{E}\{\langle X_{i-h} - \mu_{i-h}, z \rangle (X_i - \mu_i)\}$ , for all  $z \in \mathcal{H}$ . Then  $X_i \in L_{\mathcal{H}}^2$  is said to be weakly stationary if (i)  $\mathbb{E}(X_i) = \mu$  for all  $i$  and (ii)  $C_{X_{i+h}, X_{j+h}}(z) = C_{X_i, X_j}(z)$ ,  $z \in \mathcal{H}$  for all  $h$ . If  $i = j$  we write  $C_{X_i}$  instead of  $C_{X_i, X_i}$ , and  $C_{X_i, X_{i+h}} = C_h$  for weakly stationary functional time series. We observe that, if  $\{X_i\}$  is a stationary functional process, then, for any  $v \in \mathcal{H}$ , the real process  $\{\langle X_i, v \rangle\}$  is also stationary. We consider the Hilbert-Schmidt norm for covariance operators defined as  $\|C_h\|_S = \{\int_{\mathcal{T}} \int_{\mathcal{T}} \gamma_h^2(u, v) dudv\}^{1/2}$ , where  $\gamma_h(u, v) = \text{Cov}\{X_0(u), X_h(v)\}$ .

We denote by  $\mathcal{B}_{\mathcal{H}}$  the space of linear operators from  $\mathcal{H}$  to  $\mathcal{H}$  and by  $\|\cdot\|_{\mathcal{B}_{\mathcal{H}}}$  the corresponding operator norm. Let  $\{\varepsilon_i, i \in \mathbb{Z}\}$  be an i.i.d. sequence in  $L_{\mathcal{H}}^2$ , and let  $\{\Psi_i\} \in \mathcal{B}_{\mathcal{H}}$ . A functional linear process  $\{X_i, i \in \mathbb{Z}\}$  with innovations  $\{\varepsilon_i\}$  is defined as

$$X_i(s) = \sum_{j=0}^{\infty} \Psi_j(\varepsilon_{i-j})(s), \quad s \in [0, 1]. \quad (1)$$

If  $\sum_{j=0}^{\infty} \|\Psi_j\|_{\mathcal{B}_{\mathcal{H}}}^2 < \infty$ , then the series  $\{X_i\}$  is convergent in  $L_{\mathcal{H}}^2$  (Bosq, 2000). In this case, the functional linear process is stationary. The long-run covariance operator of the linear process is defined as  $V = \Psi C_{\varepsilon_0} \Psi^* \in \mathcal{B}_{\mathcal{H}}$ , where  $\Psi = \sum_{j=0}^{\infty} \Psi_j$ ,  $\Psi^*$  is the adjoint of the operator  $\Psi$ , and  $C_{\varepsilon_0}$  is the covariance operator of  $\varepsilon_0$  (see the Supplementary Material). One of the most popular models for functional time series is the functional autoregressive model of order  $p$ , FAR( $p$ ) (Horváth et al., 2010; Kokoszka and Reimherr, 2013; Aue et al., 2015). FAR( $p$ ) processes can

be seen as a particular case of a functional linear process (Bosq, 2000). We refer to Ramsay and Silverman (2005) and Bosq (2000) for a deeper understanding of functional random variables. For a comprehensive review of functional time series, unit root tests, and  $I(1)$  processes, see the Supplementary Material.

## 2.2 Depth for functional data

Several notions of functional depth have been proposed. The modified band depth (MBD) is one of the most popular functional depth and has motivated the development of extensions, modifications, and generalizations of functional depth definitions. Let  $x \in \mathcal{H}$  and let  $X$  be a functional random variable with distribution  $P$ . The MBD of  $x$  with respect to  $X$  computes the proportion of time that the curve  $x(s)$  is in a band constructed by two curves from a sample  $\{x_1, \dots, x_n\}$  of  $X \sim P$ . Then, the depth value is obtained by averaging the proportion of time over all possible bands. That is,

$$\text{MBD}(x; P) = \binom{n}{2}^{-1} \sum_{1 \leq i_1 < i_2 \leq n} \lambda[\{s \in [0, 1] \mid \min(x_{i_1}(s), x_{i_2}(s)) \leq x(s) \leq \max(x_{i_1}(s), x_{i_2}(s))\}], \quad (2)$$

where  $\lambda$  is the Lebesgue measure on  $[0, 1]$ . The definition (2) is for a band obtained with two different curves. However, the band can be obtained by more than two curves (see López-Pintado and Romo, 2009, for more details).

Another functional depth is the extremal depth (ED). The ED of  $x \in \mathcal{H}$  with respect to  $X \sim P$  computes the pointwise extremeness of the curve  $x$ . Namely, let  $S = \{x_1, \dots, x_n\}$  be a sample of  $X \sim P$ , and let  $D_x(s; S) := 1 - |\sum_{i=1}^n [\mathbf{1}\{x_i(s) < x(s)\} - \mathbf{1}\{x_i(s) > x(s)\}]|/n$  be the pointwise depth of  $x(s)$ , taking values in  $\mathbb{D} \subset \{0, 1/n, \dots, 1\}$ . Let  $G_x(r) = \int_0^1 \mathbf{1}\{D_x(s, S) \leq r\} ds$ , for each  $r \in \mathbb{D}$ , be the corresponding cumulative distribution function. Then,  $x \prec x_i$  if  $G_x(d_j) > G_{x_i}(d_j)$  for some  $j$ , with  $0 \leq d_1 < d_2 < \dots < d_M \leq 1$  the ordered elements of the depth levels obtained

from  $D_x$ . Then, the ED of  $x$  is defined as

$$\text{ED}(x; P) = 1 - \frac{\#\{i : x \prec x_i\}}{n}. \quad (3)$$

See [Narisetty and Nair \(2016\)](#) for more details.

In this paper, we do not assume any specific functional depth for the theoretical study, but we require properties to be satisfied. Here, we say that the mapping  $\text{fD} : \mathcal{H} \times \mathcal{C}(\mathcal{H}) \rightarrow \mathbb{R} : (x; P) \mapsto \text{fD}(x; P)$  is a statistical functional depth if it satisfies:

- *Nondegeneracy.* For any  $P \in \mathcal{C}(\mathcal{H})$  we have  $\inf_{x \in \mathcal{H}} \text{fD}(x; P) < \sup_{x \in \mathcal{H}} \text{fD}(x; P)$ .
- *Maximality at the center.* For any centrally symmetric  $P \in \mathcal{C}(\mathcal{H})$  we have that  $\text{fD}(z; P) = \sup_{x \in \mathcal{H}} \text{fD}(x; P)$  if and only if  $P$  is centrally symmetric around  $z \in \mathcal{H}$ .
- *Scalar-affine invariance.*  $\text{fD}(A(x); P_{A(x)}) = \text{fD}(x; P_x)$  for any  $P_x \in \mathcal{C}(\mathcal{H})$ ,  $x \in \mathcal{H}$ , and  $A : \mathcal{H} \rightarrow \mathcal{H}$  is such that  $A(x) = ax + z$  for  $x, z \in \mathcal{H}$  and  $a \in \mathbb{R} \setminus \{0\}$ .
- *Monotonicity from the center or vanishing at infinity.*  $\text{fD}$  satisfies at least one of the following:
  1. For any  $P \in \mathcal{C}(\mathcal{H})$  such that  $\text{fD}(z; P) = \sup_{x \in \mathcal{H}} \text{fD}(x; P)$  we have that  $\text{fD}(z; P) > \inf_{x \in \mathcal{H}} \text{fD}(x; P)$  and  $\text{fD}(x; P) \leq \text{fD}(z + \alpha(x - z); P)$  holds for all  $x \in \mathcal{H}$  and  $\alpha \in [0, 1]$ .
  2.  $\text{fD}(by; P) \rightarrow 0$  as  $b \rightarrow \infty$  for any  $P \in \mathcal{C}(\mathcal{H})$ , and  $y \in \mathcal{H}$  with  $y \neq 0$ .
- *Uniform continuity in  $P$ .* For all  $P, Q \in \mathcal{C}(\mathcal{H})$  and for  $\varepsilon > 0$ , there exist  $\delta > 0$  such that  $\sup_{x \in \mathcal{H}} |\text{fD}(x; P) - \text{fD}(x; Q)| < \varepsilon$  with  $d_{\mathcal{C}(\mathcal{H})}(P, Q) < \delta$ , where  $d_{\mathcal{C}(\mathcal{H})}$  metricises the topology of weak convergence.

These properties are desirable for a definition of functional depth. They hold for most known functional depths, e.g., MBD, extremal depth, and spatial depth. However, band depth ([López-Pintado and Romo, 2009](#)), the halfregion depth, and the modified halfregion depth ([López-Pintado and Romo, 2011](#)) do not satisfy all these properties. For a discussion of the above



properties and other functional depth definitions, see Nieto-Reyes and Battey (2016) and Gijbels and Nagy (2017). For illustration purposes, we will use the depths (2) and (3).

### 3 Definition of Functional Records

#### 3.1 Classical records

The classical records are defined for univariate time series. Let  $\{W_1, \dots, W_n\}$  be a sequence of continuous random variables in  $\mathbb{R}$ , and let  $W_{(1)}, \dots, W_{(n)}$  be the corresponding order statistics (observe that  $W_i = W_j$  with probability zero for  $i \neq j$ ). On this sequence, the random variable  $W_n$  is defined as an upper record if  $W_n = W_{(n)}$ , and a lower record if  $W_n = W_{(1)}$ , with probability one (Ahsanullah and Nevzorov, 2015). Finally,  $W_n$  is a record if it is a lower or upper record. When a depth notion is used, a center-outwards ordering is obtained,  $W_{[1]} \leq W_{[2]} \leq \dots \leq W_{[n]}$  with probability one, where  $W_{[i]}$  is the random variable with the  $i$ th largest depth value among the  $n$  random variables. In this case,  $W_{[n]}$  and  $W_{[n-1]}$  are the two most extreme observations. Under certain conditions on the depth (Assumption 1 below), the set of the smallest and the largest order statistics is equal to the set of the two most extreme observations, i.e.,  $\{W_{(1)}, W_{(n)}\} = \{W_{[n-1]}, W_{[n]}\}$ . Therefore, the classical records and the extreme observations identified with depth notions are equivalent. Based on these observations we extend the classical records to a generalized record definition, and we study the behavior of the number of generalized records.

#### 3.2 Functional records using depth

Suppose we observe a functional time series  $x_1(s), \dots, x_n(s)$ , at times  $i = 1, \dots, n$  with distribution  $P$ . We use functional depth to order the  $n$  curves. For each function  $x_i$ ,  $i = 1, \dots, n$ , we compute  $\text{fD}_{i,n} \in [0, 1]$  the value of the estimated functional depth among the  $n$  functions. We define an order “ $\prec$ ” among the curves as  $x_i \prec x_j$  if  $\text{fD}_{i,n} > \text{fD}_{j,n}$  and we say that  $x_j$  is more extreme than  $x_i$ . If  $\text{fD}_{i,n} = \text{fD}_{j,n}$ , i.e., if there are ties, we say that  $x_i$  and  $x_j$  are equally deep (extreme), and we use the notation  $x_i \sim x_j$ . Let  $x_{[i]}(s)$  denote the curve corresponding

to the  $i$ th largest depth value. Then,  $x_{[1]}(s), \dots, x_{[n]}(s)$  can be viewed as order statistics, with  $x_{[1]}(s)$  representing the deepest curve and  $x_{[n]}(s)$  the most outlying curve. The order statistics induced by depth start with the most central curve that corresponds to the biggest  $\text{fD}_{i,n}$  value, and move further away from the center, ending with the most extreme curve that corresponds to the smallest  $\text{fD}_{i,n}$  value.

To define functional records, we need to restrict functional depth definitions to ensure that the two most outlying curves correspond to the two most extreme curves in terms of upper and lower functional record. To clarify this idea, we consider a sequence of five functions,  $x_1(s), \dots, x_5(s)$ , in Figure 1, and we assume it is a sample functions of  $X \sim P$ . Let  $\text{fD}(x; P) = \{1 + o(x; P)\}^{-1}$  be the projection functional depth (Zuo, 2003), where  $o(x; P) = \int_0^1 \frac{|x(s) - \text{median}(X(t))|}{\text{MAD}(X(t))} ds$  is the integrated Stahel-Donoho outlyingness (Stahel, 1981; Donoho, 1982). The ordering induced by this functional depth is  $x_1 \prec x_2 \prec x_3 \prec x_4 \prec x_5$ , with  $x_4$  and  $x_5$  being the two most outlying curves. The curve  $x_5$  clearly can be considered as a record curve but not  $x_4$  among the five curves, since  $x_4$  is not an ‘‘extreme curve’’. Now, if  $\text{fD}(x; P)$  is the extremal depth or MBD, the ordering induced is  $x_1 \prec x_2 \prec x_4 \prec x_5 \prec x_3$ , with  $x_3$  and  $x_5$  being the two most outlying curves. In this case,  $x_3$  is definitely an extreme curve as well as  $x_5$ , which makes more sense in

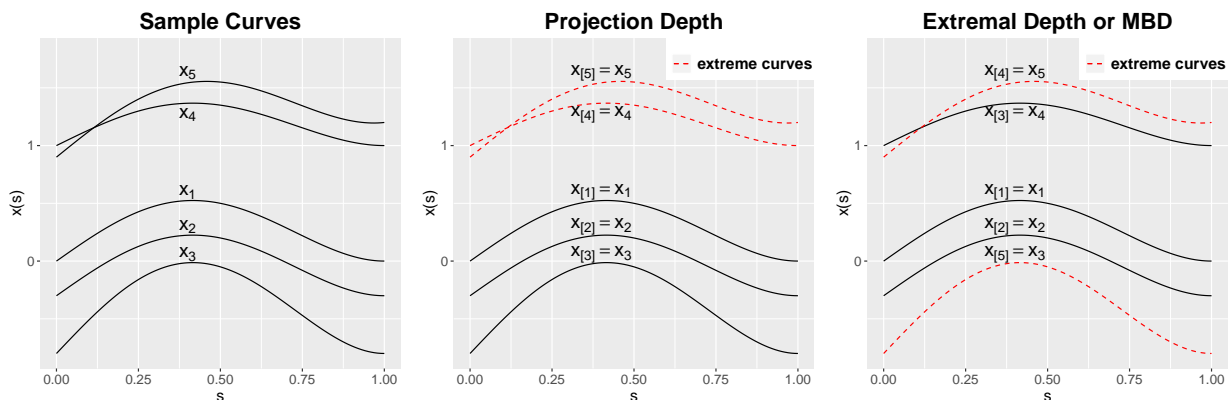


Figure 1: Two different results in the ordering of curves. Dashed curves represent the two most extreme curves. When ordering is induced by functional projection depth, the two most extreme curves are  $x_{[4]} = x_4$  and  $x_{[5]} = x_5$ . While when ordering is induced by extremal depth or MBD, the two most extreme curves are  $x_{[4]} = x_5$  and  $x_{[5]} = x_3$ .

the context of functional records. Thus, with the latter extreme curves, we can identify an upper functional record,  $x_5$ , and a lower functional record,  $x_3$  among the five curves. Without loss of generality, it is enough to verify the conditions of fD in a set of constant functions:

**Assumption 1** *Let  $a_1, \dots, a_n$  be a sequence of any real numbers with  $a_i \neq a_j$  for  $i \neq j$ , and let  $\{x_i(s) := a_i \mathbb{1}_{[0,1]}(s), i = 1, \dots, n\}$  be a sequence of functions. The functional depth fD satisfies  $\{a_{(1)} \mathbb{1}_{[0,1]}(s), a_{(n)} \mathbb{1}_{[0,1]}(s)\} = \{x_{[n]}, x_{[n-1]}\}$  as a set, where  $a_{(i)}$  is the usual order statistics.*

With this assumption, we avoid some depth definitions where the two most outlying curves are not necessarily extremes, e.g., the projection functional depth. Furthermore, if we consider the isomorphism  $a \mapsto a \mathbb{1}_{[0,1]}(s)$ , and thus assume that  $\mathbb{R} \subset \mathcal{H}$ , with Assumption 1 we obtain, as a particular case, the classical record definition. Some examples of functional depth definitions that satisfy Assumption 1 are MBD, extremal depth, and spatial depth.

In the illustration above with fD as extremal functional depth (Figure 1), the last extreme curve observed among the five curves corresponds to  $x_5$  (an upper functional record), but it does not correspond to the smallest functional depth value. The smallest functional depth value corresponds to the curve  $x_3$  (a lower functional record). In general, a new functional record does not always correspond to the smallest functional depth value, but it is one of the two smallest.

**Definition 1** *Let  $x_1, x_2, \dots$ , be an observed functional time series, and let fD be a functional depth satisfying Assumption 1. For  $j \geq 2$ , we define  $x_j$  to be a functional record if*

$$\text{fD}_{j,j} \in \{\text{fD}_{(j),j}, \text{fD}_{(j-1),j}\},$$

where  $\text{fD}_{(i),j}$  denotes the  $i$ th largest value of the functional depths among  $\{x_1, \dots, x_j\}$ .

The nondegeneracy of functional depth is important in the functional record definition, because if the functional depth definitions suffer a degeneracy problem, i.e., with probability one the depth value is zero for every function in a general class of continuous Gaussian processes (Chakraborty and Chaudhuri, 2014a), then each function can be a functional record.

**Remark 1** *The functional record definition represents both the upper and lower records. This is because depth is a centrality measure, and thus we are not able to identify whether  $x_{[j],j}$ , among  $x_1, \dots, x_j$ , corresponds to an upper or a lower extreme curve.*

Once a functional record  $x_j$  is observed at time  $j$ , it may be visually easy to classify as upper or lower functional records. One way to define upper and lower functional record is using the deepest curve (median curve) as a reference curve, and computing the proportion  $T_j^u$  of time that  $x_j$  is above the median curve and the proportion  $T_j^l$  of time that  $x_j$  is below the median curve. In Figure 1 with extremal depth,  $x_1$  is the deepest curve, and  $T_5^u = 1$  and  $T_5^l = 0$ , whereas  $T_3^u = 0$  and  $T_3^l = 1$ . Thus, we say that  $x_5$  is an upper functional record since  $T_5^u > T_3^u$ . Definition 2 formalizes this idea.

**Definition 2** *Let  $x_j$  be a functional record according to Definition 1. We say that  $x_j$  is an upper record if  $\int_0^1 \mathbb{1}\{s : x_j(s) \geq x_{[1],j}(s)\} ds > \int_0^1 \mathbb{1}\{s : x_j(s) < x_{[1],j}(s)\} ds$ , and a lower record in the other case.*

In general, it is unlikely to observe ties in the depth values, i.e., that  $\text{fD}_{i,n} = \text{fD}_{j,n}$  for some  $i, j \in \{1, \dots, n\}$  and  $i \neq j$ . However, it does not have a zero probability, especially for small sample sizes and functional depths taking values of the form  $1/j$ ,  $j = 1, \dots, n$ . We observe that ties do not affect Definition 1 unless it occurs with the last two smallest functional depth values,  $\text{fD}_{n-1,n}$  and  $\text{fD}_{n,n}$ . Let  $x_j$  be the last functional record observed at time  $n-1$ , i.e., among  $\{x_1, \dots, x_{n-1}\}$ . According to Definition 1, if  $\text{fD}_{n,n} = \text{fD}_{j,n}$ , then  $x_n$  is a new functional record at time  $n$ . Thus, unlike the classical record definition in  $\mathbb{R}$ , we define  $x_n$  as a functional record if it is equally extreme as the previous two most extreme curves at time  $n-1$ . Moreover,  $x_n(s) = x_j(s)$  with probability zero if  $P_{X(s)}$  is a continuous distribution function.

Ties can be broken by using an auxiliary sequence of i.i.d. random variables  $W_i$ ,  $i = 1, \dots, n$ , such that  $W_1$  has an absolutely continuous distribution and independent of  $P$  (see, e.g., Dufour, 2006). Then a strict and total order can be obtained as follows:  $(x_i, W_i) \prec (x_j, W_j)$  if and only if  $\text{fD}_{i,n} > \text{fD}_{j,n}$  or if  $\text{fD}_{i,n} = \text{fD}_{j,n}$  and  $W_i > W_j$ .

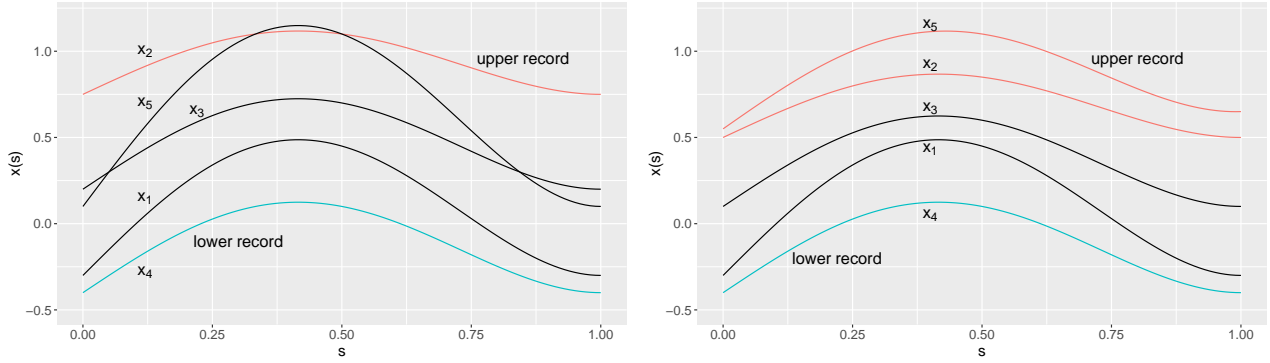


Figure 2: Functional records with  $n = 5$  curves. The upper functional record is indicated by the red curve, and the lower functional record is indicated by the blue curve. Left: the last functional record observed is  $x_4$  and corresponds to the lower functional record. Right: the last functional record observe is  $x_5$  and corresponds to the upper functional record.

Figure 2 shows an example of the functional record definition with  $n = 5$ . Here, we use MBD to compute the functional records (a similar result is obtained with extremal depth). In the left plot, we obtain two functional records, at  $j = 2$  and  $j = 4$  ( $x_2$  is a functional record by definition), corresponding to the upper functional record and the lower functional record, respectively. The curve  $x_4$  is the last functional record observed since  $x_5$  is deeper than  $x_2$  and  $x_4$  in the sample. In contrast, in the right plot, we obtain three functional records,  $x_2$ ,  $x_4$ , and  $x_5$ , where  $x_2$  and  $x_5$  are upper functional records at times  $j = 2, 5$ , respectively, and  $x_4$  is a lower functional record. In this case,  $x_5$  is the last functional record observed, since  $x_2$  is now deeper than  $x_4$  and  $x_5$  in the sample. In this last case, we obtain ties in the last two extreme curves, i.e.,  $\text{fD}_{4,5} = \text{fD}_{5,5}$ . However, these curves are on opposite sides of the sample, hence it makes sense to define  $x_5$  as a new functional record. Now, if one considers the auxiliary variables  $W_i$  to break ties, the result does not change, either  $x_4 \prec x_5$  or  $x_4 \succ x_5$ , since  $\text{fD}_{5,5} \in \{\text{fD}_{4,5}, \text{fD}_{5,5}\}$ .

## 4 Properties of Functional Record Number

Let  $\{X_i(s), i \geq 1\}$  be a sequence of functional random variables with distribution  $P$ . Let  $\text{fD}(x; P)$  be a functional depth that satisfies Assumption 1. For  $j \geq 2$ , let  $X_{[1],j}(s), \dots, X_{[j],j}(s)$  be the

order statistics induced by the functional depth fD for the first  $j$  functional random variables. Then,  $X_j$  is defined as a functional record at time  $j$  if

$$X_j \in \{X_{[j-1],j}(s), X_{[j],j}\}. \quad (4)$$

For  $i = 1, \dots, j$ , we define  $T_{i,j}^u$  as the proportion of time at which  $X_i$  is above the central curve  $X_{[1],j}$ ,  $T_{i,j}^u := \int_0^1 \mathbf{1}\{s : X_i(s) \geq X_{[1],j}(s)\} ds$ , and  $T_{i,j}^l := \int_0^1 \mathbf{1}\{s : X_i(s) < X_{[1],j}(s)\} ds$  as the proportion of time at which  $X_i$  is below  $X_{[1],j}$ . If  $X_j$  is a functional record at time  $j$ , we say that  $X_j$  is an upper functional record if  $T_{j,j}^u > T_{j,j}^l$ , and a lower functional record otherwise.

We study the number of functional records over time. Let  $R_j = \mathbf{1}\{X_j \text{ is a functional record}\}$  be the indicator of  $X_j$  being a functional record at time  $j$ , and let  $N_j$  be the counting process representing the number of functional records among  $X_1, \dots, X_j$ , i.e.,

$$N_j = \sum_{i=1}^j R_i, \quad (5)$$

where  $R_1 := 1$ . We define the functional record times as  $L(1) = 1$ ,  $L(2) = 2$ , and for  $k = 3, 4, \dots$ ,  $L(k) = \min\{j : j > L(k-1) \text{ and } R_j = 1\}$ . We use the notations  $R_j^u, N_j^u$ , and  $L^u(k)$  to denote the respective variables for the upper functional records. Observe that a lower functional record is an upper functional record of the process  $\{-X_i\}$ . Therefore, we focus on the upper functional records. To establish the theoretical properties of the process  $N_n^u$ , we assume the following:

**Assumption 2** *Let  $\{X_1, X_2, \dots, X_j\}$  be a sequence of functional random variables, with  $j \geq 3$ . If  $R_j = 1$ , then, with probability one*

$$\max\{\text{fD}(X_j; P); \text{fD}(X_{L^u(j-1)}; P), \text{fD}(X_{L^l(j-1)}; P)\} < \min\{\text{fD}(X_i; P); i \in \{1, \dots, j-1\} \setminus \{L^u(j-1), L^l(j-1)\}\}.$$

Assumption 2 means that ties are allowed, but if  $X_j$  is a functional record at time  $j$  then  $X_j$  can only tie with curves in  $\{X_{L^u(j-1)}, X_{L^l(j-1)}\}$ . Also, with Assumption 2, it is not possible to observe more than one upper (lower) functional record at time  $j$ .

In the univariate case, it is known that if the time series is an independent sequence or a stationary time series satisfying the Berman condition, then  $N_j^u$  grows at rate  $\log j$  (Lindgren

and Rootzén, 1987). On the other hand, if the time series is a random walk process, then the growth rate of  $N_j^u$  is  $j^{1/2}$  (Sparre Andersen, 1954; Feller, 1971; Burridge and Guerre, 1996). With the previous definitions, we show similar results for functional records.

We observe that, if  $\{X_i\}$  is an independent sequence in  $\mathcal{H}$ , then  $P(R_j^u = 1) = 1/j$  for any ranking definition. Indeed, the probability of  $X_j$  being a record is the probability of  $X_j$  taking a specific place among  $\{1, \dots, j\}$ . Then,  $N_j^u = O(\log j)$  with probability one.

**Proposition 1** *Let  $\{X_i\}$  be a stationary functional time series such that  $\log(h)\|C_h\|_S \rightarrow 0$  as  $h \rightarrow \infty$ . Let  $\text{fD}$  be a functional depth that satisfies Assumption 1. Then, under Assumption 2*

$$\frac{N_n^u}{\log n} = O(1),$$

with probability one, when  $n \rightarrow \infty$ .

The proof of Proposition 1 is based on the dependency structure of the sequence of random variables,  $\{X_1, X_2, \dots\}$ , independently if they take values in real numbers or function space (see Lindgren and Rootzén, 1987).

The condition on the covariance operator in Proposition 1 is not restrictive for functional time

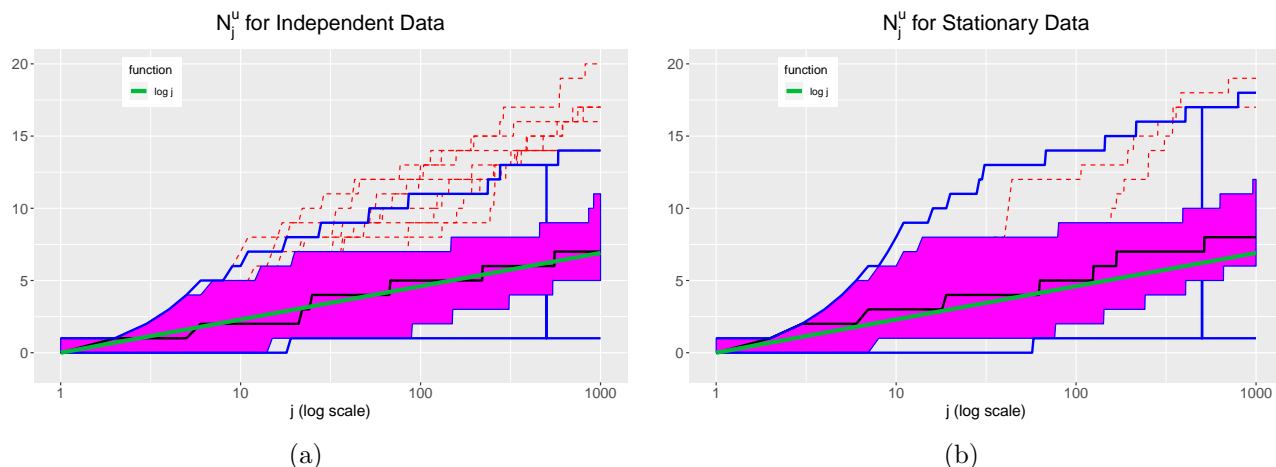


Figure 3: Log scale functional boxplot of 1000 trajectories of  $N_j^u$  by using MBD with  $j = 2, \dots, 1000$ . Each trajectory of  $N_j^u$  is obtained from  $\{X_i\}_{i=1}^n$  where  $n = 1000$ , and  $\{X_i\}$  is an independent functional sequence (left) and a stationary functional sequence (right). The green curve represents the  $\log j$  function.

series, and it holds if the functional time series is  $L^2$ - $m$ -approximable (Hörmann and Kokoszka, 2010). Hörmann and Kokoszka (2010) showed that this approximation is valid for linear and non-linear functional time series. In particular, the FAR(1) model with coefficient operator that has norm less than one is  $L^2$ - $m$ -approximable.

We simulate  $X_i = \varepsilon_i, i = 1, \dots, n = 1000$  as an independent sequence, where, for each  $i$ ,  $\varepsilon_i$  is a Brownian motion in  $[0, 1]$ . Figure 3(a) shows the functional boxplot (Sun and Genton, 2011) of 1000 trajectories of  $N_j^u$  with  $j = 2, \dots, n$ , using the modified band depth (MBD) on the independent sample curves. In Figure 3(b), we simulate stationary functional time series from  $X_i(s) = c_1 \int \beta(t, s) X_{i-1}(t) dt + \varepsilon_i(s)$ , where  $\beta(t, s) = \exp\{-(t^2 + s^2)/2\}$ , and  $c_1$  is such that  $\{\int \int c_1^2 \beta(t, s)^2 dt ds\}^{1/2} = 0.5$ . We observe that  $N_j^u$ , in both cases, has the same growth rate, i.e.,  $\log j$ .

Now, we state the result for  $N_j^u$  under a nonstationary functional process.

**Proposition 2** *Let  $X_i = X_{i-1} + \varepsilon_i$  be a functional random walk with  $\{\varepsilon_i\}$  an i.i.d. sequence in  $L_{\mathcal{H}}^2$ . If  $\varepsilon_0$  has a symmetric distribution about the mean, and the functional depth FD satisfies Assumption 1, then, under Assumption 2*

$$\frac{N_n^u}{\sqrt{n}} \xrightarrow{d} G_1, \quad (6)$$

when  $n \rightarrow \infty$ , where  $G_1$  is a random variable with probability density function  $g_1(x) = \frac{1}{\sqrt{\pi}} \exp(-x^2/4)$  for  $x \geq 0$ .

Proof: See Appendix.

Proposition 2 can be generalized to  $I(1)$  functional processes (see Section 5). As an illustration of the result in Proposition 2, we simulate a functional random walk, with Brownian motion in  $[0, 1]$ , as a functional white noise, and for different sample sizes  $n = 100, 1000$  and  $10000$ . We simulate 1000 replicates of each case, and then obtain 1000 replicates of  $N_n^u$ . Figure 4 shows histograms of  $N_n^u/\sqrt{n}$  where the solid blue curve represents the asymptotic distribution from Proposition 2. We observe that the asymptotic distribution provides a better description of the



empirical distribution when the sample size increases. However, with a sample size  $n = 100$ , this approximation is already reasonably good.

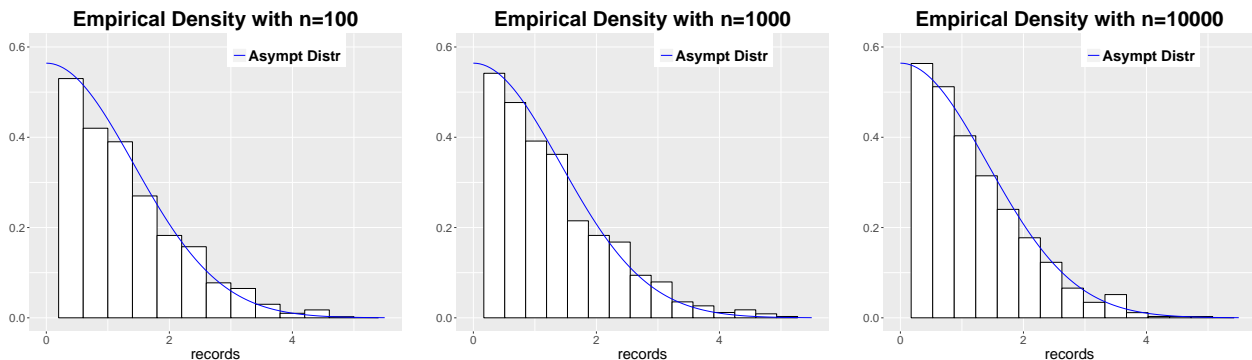


Figure 4: Histogram of  $N_n^u$  with  $n = 100, 1000, 10000$ , and the asymptotic distribution (solid blue curve) from Proposition 2.

## 5 Application to Functional Unit Root Test

Records have been used in different problems, in particular to test for a unit root (see [Burrige and Guerre, 1996](#); [Aparicio et al., 2006](#)). In real data applications, a functional unit root could arise alike the univariate unit root processes. Assume that our functional data satisfy the random walk model  $X_i(s) = X_{i-1}(s) + \varepsilon_i(s)$  with  $i$  representing years, and  $s$  the day index within a year. Let  $W_j = \frac{1}{365} \sum_{s=1}^{365} X_j(s)$  be the annual mean of the functional time series  $X_j$ . We observe that  $\{W_j\}$  has also a unit root, i.e.,  $W_i = W_{i-1} + \tilde{\varepsilon}_i$ . This is caused by the unit root in the functional time series. A unit root test can be applied to the annual time series  $\{W_j\}$ . However, we cannot guarantee the presence of a unit root for each day within the year. If we do not aggregate the data and consider a longer univariate time series as  $\{X_1(1), X_1(2), \dots, X_1(365), X_2(1), \dots, X_2(365), X_3(1), \dots\}$ , the unit root might then be undetectable, since  $X_i(s)$  is not necessarily equal to  $X_i(s-1) + \varepsilon_i(s)$ . Functional data analysis deals with this problem, assuming the whole observations during the year as a single object, and taking into account the information within the year.

In this section, we propose a unit root test for functional time series that uses the normalized

counting process  $N_n = N_n^u + N_n^l$ . One advantage of using records to test for a unit root is that it is a nonparametric test; it is also robust against structural breaks, and it does not involve the estimation of any coefficient operators that could be a difficult task and therefore face computational issues. Moreover, a unit root test based on records is invariant under monotonic transformations of the data, since records are invariant too. Thus, we can use records to test a unit root in a general class of  $I(1)$  functional processes.

## 5.1 $I(1)$ functional processes

One can define an  $I(1)$  functional process by projecting the functional time series on  $v \in \mathcal{H}$ , and by applying the univariate definition. This means that we assume  $\{X_i, i \geq 0\}$  to be an  $I(1)$  functional process if there exist a  $v \in \mathcal{H}$  such that  $\{\langle X_i, v \rangle, i \geq 0\}$  is a univariate  $I(1)$  process in  $\mathbb{R}$ . This definition was used in [Muriel \(2015\)](#) who called  $v$  a “weak unit root”. Another extension of the definition of  $I(1)$  functional process involves the use of the Johansen approach ([Beare et al., 2017](#)). Assume that  $\{X_i\}$  is a functional linear process such that the first difference  $\Delta X_i := X_i - X_{i-1}$  admits the functional linear representation in (1) with innovations  $\{\varepsilon_i\}$ , i.e.,  $\Delta X_i = \sum_{j=0}^{\infty} \Phi_j(\varepsilon_{i-j})$ , where  $\{\Phi_j\} \in \mathcal{B}_{\mathcal{H}}$ , and  $\sum_{j=0}^{\infty} j \|\Phi_j\|_{\mathcal{B}_{\mathcal{H}}} < \infty$ . Let  $C_{\varepsilon_0}$  be the covariance operator of  $\varepsilon_0$  that is positive definite, and denote by  $\Lambda = \Phi C_{\varepsilon_0} \Phi^*$  the long-run covariance operator of  $\{\Delta X_i, i \geq 1\}$ , with  $\Phi = \sum_{i=0}^{\infty} \Phi_i$ . Then,  $\{X_i, i \geq 0\}$  can be written as

$$X_i(s) = Z_0(s) + \Phi \left( \sum_{j=1}^i \varepsilon_j \right) (s) + \eta_i(s), \quad (7)$$

where  $Z_0 \in L_{\mathcal{H}}^2$ , and  $\{\eta_i\}$  is a weakly stationary process in  $\mathcal{H}$ . The solution (7) contains an initial condition  $Z_0$ , a functional random walk component  $\Phi(\sum_{j=1}^i \varepsilon_j)$ , and a stationary component  $\eta_i$ . Observe that the functional random walk component is defined only on  $\text{ran } \Phi = \{\Phi(z) : z \in \mathcal{H}\}$ , thus the functional time series is stationary on the complementary space. Then,  $\{X_i\}$  is an  $I(1)$  functional process if, and only if,  $\Lambda \neq 0$  ([Beare et al., 2017](#)). In this paper, we adopt this last definition.

**Example 1 (FAR(1))** Assume that  $\{X_i\}$  is a FAR(1) process,  $X_i(s) = \rho_1(X_{i-1})(s) + \varepsilon_i(s)$ .

1. If  $\rho_1 = \text{Id}_{\mathcal{B}\mathcal{H}}$ , where  $\text{Id}_{\mathcal{B}\mathcal{H}}$  denotes the identity operator from  $\mathcal{H}$  to  $\mathcal{H}$ , then  $X_i$  is a functional random walk and can be written as

$$X_i(s) = X_0(s) + \sum_{j=0}^i \varepsilon_{i-j}(s).$$

Therefore  $\{X_i\}$  is an  $I(1)$  functional process.

2. If  $\rho_1 \neq \text{Id}_{\mathcal{B}\mathcal{H}}$  and  $\rho_1$  is a compact operator with one eigenvalue equal to one, that is, there exist  $v \in \mathcal{H}$  such that  $\rho_1(v) = v$ , then the operator pencil  $A(z) = \text{Id}_{\mathcal{H}} - z\rho_1$  is not invertible at  $z = 1$ . Moreover, the space  $\mathcal{H}$  can be decomposed as  $\mathcal{H} = \text{ran } A(1) \oplus \text{ker } A(1)$ , such that  $\{\langle X_i, z \rangle\}$  is a univariate  $I(1)$  process for all  $z \in \text{ran } A(1)$ , and  $\{\langle X_i, z \rangle\}$  is stationary for all  $z \in \text{ker } A(1)$ . As a consequence,  $X_i$  can be written as in (7), and therefore  $\{X_i\}$  is an  $I(1)$  functional process.

Under the FAR(1) model (or FAR( $p$ ) model), the presence of a unit root affects the accuracy of the estimation of the coefficient operator  $\rho_1$ . Most of the properties of existing estimators will not hold, and we need to consider an alternative model. Therefore, a functional unit root has an impact on both estimation and modeling. Thus, we need to detect the unit root accurately.

## 5.2 Functional records for $I(1)$ processes

One advantage of using a depth notion for a functional unit root test is that the functional depth is computed in the stationary subspace with probability zero, in other words, the extreme curves correspond to a functional random walk process with probability one. We show this in the following proposition.

**Proposition 3** Let  $\{X_i\}$  be an  $I(1)$  functional process in  $\mathcal{H}$ . Assume  $\{\varepsilon_i\}$  is an i.i.d. sequence in  $L^2_{\mathcal{H}}$  with symmetric distribution about the mean, and the functional record fD satisfies Assumption 1. Then, under Assumption 2, the corresponding counting process  $N_n^u$  for  $\{X_i\}_{i=1}^n$  has

the same asymptotic distribution as the corresponding counting process for a functional random walk in Proposition 2.

Proof: See Appendix.

*Record-based (RB) Functional Unit Root Test.* We consider the testing of the null hypothesis of an  $I(1)$  functional process versus the functional process is stationary. In other terms,

$$H_0 : X_i \text{ is an } I(1) \text{ functional process vs } H_1 : X_i \text{ is a stationary process,}$$

where the corresponding innovations  $\{\varepsilon_i\}$  are assumed to be symmetrically distributed. The test statistic  $T_n$  for the RB-functional unit root test is the number of upper and lower records normalized with  $\sqrt{n}$ , i.e.,  $T_n = n^{-1/2}N_n = n^{-1/2}(N_n^u + N_n^l)$ .

**Corollary 1** *Let  $\{X_i\}$  be a functional linear process with innovations  $\{\varepsilon_i\}$  having a symmetric distribution about the mean, and let fD be a functional record satisfying Assumption 1. Then, under Assumption 2, it holds that*

1. *under the null hypothesis,  $T_n \xrightarrow{d} G_2$ , where  $G_2$  is a random variable with probability density function  $g_2(x) = \sqrt{\frac{2}{\pi}}x^2 \exp(-x^2/2)$ ,  $x \geq 0$ , and*
2. *under the alternative hypothesis,  $T_n \xrightarrow{p} 0$ .*

Proof: See Appendix.

From Corollary 1, we use the left tail of the asymptotic distribution of the test statistic  $T_n$  to test for a functional unit root, i.e., given the significance level  $\alpha$ , reject  $H_0$  if  $T_n$  is smaller than the quantile  $q_\alpha$  of  $g_2(x)$ , where  $q_\alpha$  is the quantile of order  $\alpha$  of  $g_2(x)$ .

In the following sections, we present a Monte Carlo simulation study to evaluate the performance of the test for a finite sample size.

### 5.3 Simulation design

We study the performance of the unit root test, based on functional records under the null and alternative hypothesis. We simulate different functional time series,  $\{X_i(s)\}_{i=1}^n$ , at 50 points equispaced on  $[0, 1]$  with the different sample sizes  $n = 200, 300, 500$  and 1000. Each scenario is replicated 1000 times. Let  $\{\varepsilon_i(s)\}$  be a sequence of independent functional random variables. We consider the following models:

1.  $X_i(s) = X_{i-1}(s) + \varepsilon_i(s)$ ;
2.  $X_i(s) = \rho(X_{i-1})(s) + \varepsilon_i(s)$ , where  $\rho(z)(s) = a(\langle z, e_1 \rangle + \langle z, e_2 \rangle)e_1(s) + a\langle z, e_1 \rangle e_2(s)$ ,  $\{e_1, e_2\}$  is an orthonormal basis function, and  $a = -1/2 + \sqrt{5}/2$ . Assuming that the white noise  $\{\varepsilon_i\}$  satisfies  $\mathbb{E}(\langle \varepsilon_i, e_1 \rangle^2) > 0$  but  $\mathbb{E}(\langle \varepsilon_i, e_2 \rangle^2) = 0$ ;
3.  $X_i(s) = \varepsilon_i(s)$ ;
4.  $X_i(s) = \Psi_1(X_{i-1})(s) + \varepsilon_i(s)$ , where  $\Psi_1(z) = c_1 \int_0^1 \exp\{(u^2 + s^2)/2\}z(u)du$  and  $c_1$  is such that  $\|\Psi_1\|_{\mathcal{B}_H} = 0.5$ ;
5.  $X_i(s) = \mu_1(s)\mathbb{1}_{\{i \leq k\}} + \mu_2(s)\mathbb{1}_{\{i > k\}} + \eta_i(s)$ , where  $\eta_i(s)$  is a stationary FAR(1) process as in Model 4,  $\mu_1(s) = 0$ ,  $\mu_2(s) = 2$  and  $k = n/2$ ; and
6.  $X_i(s) = (\Psi_1\mathbb{1}_{\{i > k\}} + \Psi_2\mathbb{1}_{\{i \leq k\}})(X_{i-1})(s) + \varepsilon_i(s)$ , where  $\Psi_1$  is as in Model 4 and  $\Psi_2(z) = c_2 \int_0^1 \exp\{-(u^2 + s^2)/2\}z(u)du$  where  $c_2$  is such that  $\|\Psi_2\|_{\mathcal{B}_H} = 0.7$ , and  $k = n/2$ .

The choice of the parameter  $a$  in Model 2 makes  $\rho$  an operator with an eigenvalue equal to one and the rest has modulus less than one. Models 1 and 2 are under the null hypothesis, i.e.,  $\{X_i\}$  is an  $I(1)$  functional process, whereas, in Models 3 to 6,  $\{X_i\}$  is not an  $I(1)$  functional process. Particularly, in Models 3 and 4,  $\{X_i\}$  is stationary. We consider the functional white noise to be the Brownian motion (Bm),  $\varepsilon_i(s) = W_i(s)$ ,  $s \in [0, 1]$ , the Brownian bridge (Bb),  $\varepsilon_i(s) = W_i(s) - sW_i(1)$ ,  $s \in [0, 1]$ , and  $\varepsilon_i(s)$  as a stochastic Gaussian process (Gp(0,  $\gamma$ )) with zero mean and covariance function  $\gamma(s, t) = 0.2 \exp\{-0.3|s - t|\}$  in  $[0, 1]$ .

For comparison, we adopt the regression approach to mimic the Dickey-Fuller test (Dickey and Fuller, 1979). We fit the model  $X_i(s) = \int_{[0,1]} \beta(t,s) X_{i-1}(t) dt + \omega_i(s)$  for each simulated functional time series, where  $\beta(t,s)$  is estimated using a penalized least square estimator (Martínez-Hernández et al., 2019). We then compute the corresponding norm of the coefficient operator,  $\{\int \int \beta^2(t,s) dt ds\}^{1/2}$ . If  $\{X_i\}$  is an  $I(1)$  functional process, we expect the norm to be close to one, and if  $\{X_i\}$  is stationary, we expect the norm to be smaller than one. We report the mean norm values over replicates.

## 5.4 Empirical size and power of the test

We compute the test statistic  $T_n$  by using MBD, and we compare it with the quantile  $q_{0.05}$  obtained from the asymptotic distribution in Corollary 1. Table 1 presents the proportion of rejections when the functional time series is under the null hypothesis. We expect these values to be close to the significance level 0.05. We observe that, for Model 1 with white noise Bm, the proportion of rejection is 0.017 when  $n = 200$ , and it increasing to 0.027 when  $n = 1000$ . We observe similar results when the white noise is Bb. This suggests a slow rate of convergence to the left tail of the asymptotic distribution. In general, the proportion of rejections gets closer

Table 1: Empirical size. Proportion of rejections under the null hypothesis. We simulate functional time series from Models 1 and 2 with different functional white noises, Brownian motion (Bm), Brownian bridge (Bb), and Gaussian process with zero mean and covariance function  $\gamma$  (Gp(0,  $\gamma$ )). The sample sizes considered are  $n = 200, 300, 500$  and 1000. Each scenario is replicated 1000 times. The values in parentheses indicate the mean value of the norm of the coefficient operator in the FAR(1) model. Nominal level is 5%.

$n$	Model 1				Model 2			
	200	300	500	1000	200	300	500	1000
$\varepsilon_i$								
Bm	0.017 (1.615)	0.024 (1.660)	0.017 (1.648)	0.027 (2.131)	0.011 (1.238)	0.013 (1.660)	0.005 (1.719)	0.005 (1.905)
Bb	0.002 (1.711)	0.001 (1.809)	0.002 (1.683)	0.004 (1.835)	- (-)	- (-)	- (-)	- (-)
Gp(0, $\gamma$ )	0.026 (1.767)	0.043 (1.526)	0.043 (1.826)	0.050 (1.750)	- (-)	- (-)	- (-)	- (-)

to the chosen significance level as the sample size increases. In contrast, when the functional white noise is  $Gp(0, \gamma)$ , we observe a faster convergence of the proportion of rejections to the significance level. For Model 2, there is only one white noise because of the restriction on the model. In this case, the proportion of rejections is similar to that in Model 1 with white noise Bb. With respect to the norm values indicated in parentheses, we observe mean values bigger than one, in all cases. This means, the fitted FAR(1) model is a nonstationary functional time series, in agreement with the data generating processes.

Our next step is to study the power of the test. Table 2 presents the proportion of rejections under the alternative. Note that Model 3 represents a stationary, independent sequence of functional data, whereas Model 4 represents stationary, dependent functional data. In Model 3, the proportion of rejections is bigger than 0.95 for small sample sizes, independently of the selection of the white noise  $\varepsilon_i$ . In Model 4, the proportion of rejections is bigger than 0.97 for sample sizes bigger than  $n = 300$ . In general, the test shows a high power, even for the smaller sample size,  $n = 200$ . For norm values, we observe that the respective means of the norms for Models 3 and 4 are approximately 0.1 and 0.5, for all cases. This means that the fitted FAR(1) model is a stationary functional time series, and that the mean norm agrees with the norm of

Table 2: Empirical power. Proportion of rejections under the alternative hypothesis. Functional time series are simulated from Models 3 and 4 with different functional white noises, Brownian motion (Bm), Brownian bridge (Bb), and Gaussian process with zero mean and covariance function  $\gamma$  ( $Gp(0, \gamma)$ ). The sample sizes considered are  $n = 200, 300, 500$  and  $1000$ . Each scenario is replicated 1000 times. The values in parentheses indicate the mean value of the norm of the coefficient operator in the FAR(1) model.

	Model 3				Model 4			
$n$	200	300	500	1000	200	300	500	1000
$\varepsilon_i$								
Bm	0.956 (0.125)	0.997 (0.121)	1.000 (0.107)	1.000 (0.086)	0.894 (0.475)	0.981 (0.488)	0.998 (0.497)	1.000 (0.503)
Bb	0.968 (0.117)	0.999 (0.104)	1.000 (0.093)	1.000 (0.069)	0.888 (0.461)	0.972 (0.474)	0.999 (0.484)	1.000 (0.490)
$Gp(0, \gamma)$	0.966 (0.151)	0.994 (0.141)	1.000 (0.126)	1.000 (0.102)	0.913 (0.502)	0.982 (0.516)	0.999 (0.518)	1.000 (0.517)

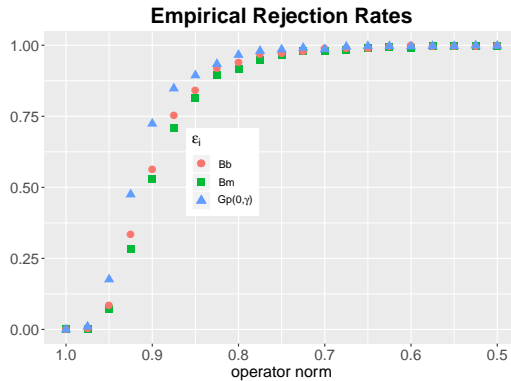


Figure 5: Rejection rate for different operator norms of the coefficient operator in Model 4.

the data generating processes.

Also, we investigate the power curve for Model 4 when we vary the operator norm  $\|\Psi_1\|_{\mathcal{B}_H} = 0.5, 0.525, \dots, 0.975, 1$ . Figure 5 shows the rejection rate at level  $\alpha = 0.05$  with  $n = 500$  for each different operator norm. We observe that the test has good power, correctly rejecting the null hypothesis when operator norms are smaller than 0.9. As a conclusion, the RB-functional unit root test shows an accurate balance of the significance level and power of the test, already for a medium sample size ( $n = 300$ ).

### 5.5 Robustness against structural changes

One of the advantages of using functional records in the hypothesis test is the robustness to different nonstationary models. Models 5 and 6 represent unstable time series, with change on the mean, and change on the coefficient operator, respectively. However, Models 5 and 6 are not  $I(1)$  functional processes, so we expect to reject  $H_0$ . The counting processes  $N_j$  for Models 5 and 6 should grow at the same rate as that in the stationary case:  $N_j = O(\log j)$ . Table 3 shows the corresponding proportion of rejections for these models.

For Model 5, we observe a low proportion of rejections, when the sample size is smaller than 500, but the results improve for  $n > 500$ . Thus, the test requires a sample size bigger than 500, for a reasonable power. For Model 6, the results are different. We observe that, for  $n = 200$ , the proportion of rejections of the null hypothesis is bigger than 0.7, for white noises Bm and Bb,



Table 3: Proportion of rejections against models with structural changes. Functional time series are simulated from Models 5 and 6 with different functional white noises, Brownian motion (Bm), Brownian bridge (Bb), and Gaussian process with zero mean and covariance function  $\gamma$  (Gp(0,  $\gamma$ )). The sample sizes considered are  $n = 200, 300, 500$  and 1000. Each scenario is replicated 1000 times. The values in parentheses indicate the mean value of the norm of the coefficient operator in the FAR(1) model.

$n$	Model 5				Model 6			
	200	300	500	1000	200	300	500	1000
$\varepsilon_i$								
Bm	0.195 (0.989)	0.391 (1.001)	0.657 (1.013)	0.975 (1.023)	0.709 (0.579)	0.886 (0.598)	0.983 (0.615)	1.000 (0.631)
Bb	0.134 (0.953)	0.321 (0.957)	0.571 (0.960)	0.956 (0.963)	0.707 (0.575)	0.923 (0.592)	0.983 (0.603)	1.000 (0.613)
Gp(0, $\gamma$ )	0.460 (0.945)	0.658 (0.957)	0.842 (0.969)	0.995 (0.979)	0.815 (0.617)	0.937 (0.628)	0.991 (0.636)	1.000 (0.643)

and bigger than 0.8, for a white noise Gp(0,  $\gamma$ ). We obtain a proportion of rejections bigger than 0.88, when  $n \geq 300$ . In general, the RB-functional unit root test is robust against structural changes, although a bigger sample size is needed when changes occur on the mean. In contrast, we observe that the norm of the coefficient operator is affected by structural changes. In particular, for Model 5, we obtain a mean value of the norms close to one, indicating the possible existence of a unit root on the data generating processes. In general, we conclude that a test based on regression will have low power in the presence of a structural change, similarly to what occurs with univariate time series.

Our test does not depend on a specific model, and is invariant under monotonic transformations. It is expected to have a good performance, with a broad class of models, and in practice, the computation of the number of functional records does not depend on the depth definition.

## 6 Data Applications

We study the behavior of functional records in two different datasets, and apply the RB-functional unit root test. First, we consider daily curves of the hourly wind speed taken at Yanbu, Saudi Arabia. Our second example involves the annual mortality rates in France (from the R package

demography), from 1816 to 2006. We consider the MBD to compute the functional record curves.

## 6.1 Wind speed in Saudi Arabia

The dataset consists of  $n = 755$  daily curves of wind speed, at Yanbu, Saudi Arabia, from August 30, 2014 to September 22, 2016. Each point of the curve represents wind speed at 80m [ $m/s$ ]. The study of the behavior of the wind speed is important for renewable energy generations. Particularly, by knowing when and how often a record curve of wind speed is observed, we can describe the dynamics of the extreme wind speed curves. An accurate characterization of the extreme daily curves is crucial to predict the efficiencies of wind turbines and energy storage in the presence of an extreme event.

We exclude the two first curves that are functional records by definition. We found that the functional records for 2014 are: Sept. 5, 12, 14, 17, 25, 26, 30, Oct. 5, 8, 9, 10, and Nov. 20. The record curves for 2015 are: Mar. 2, 4, Apr. 17, 24, May 15, and June 05, 06. The record curves for 2016 are: July 23, and Sept. 5. Figure 6 shows the wind speed curves together with the functional records. On the left, we plot the 755 wind speed curves; those curves that are not classified as records are indicated in gray. The functional records are plotted from white to red (heat colors), according to the order in which they appear. In this dataset, the functional records correspond to lower wind speeds at the beginning, and higher wind speeds at the end.

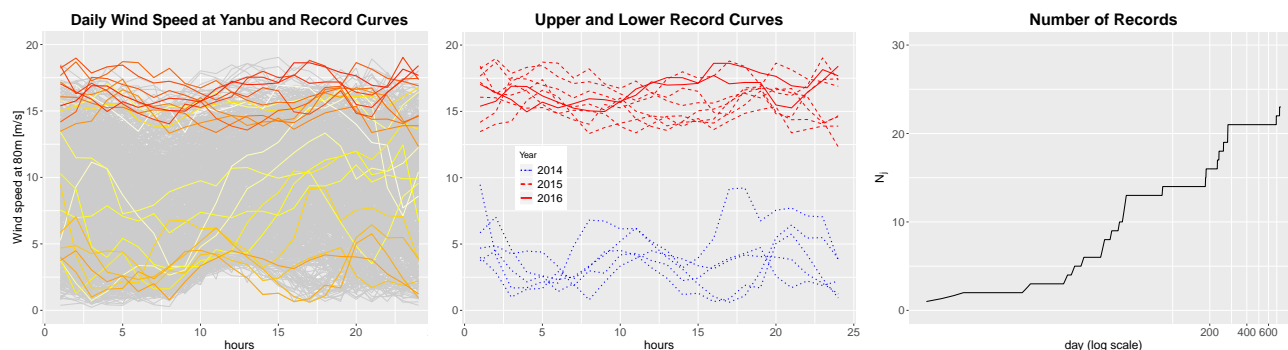


Figure 6: Left: Data of daily wind speed at Yanbu, Saudi Arabia, from August 30, 2014 to September 22, 2016. Center: Lower records in blue color and upper records in red color. Right: Trajectory of the number of functional records  $N_j$ ,  $j = 2, \dots, 755$ .

To have a better visualization of the results, we plot the functional records on the center of Figure 6. The first seven record curves that correspond to September can be considered as part of the inherent variability of the functional process, so we do not include them in the plot. The lower functional records are indicated by the blue curves, and the upper functional records are indicated by the red curves. We indicate the corresponding year by using different line types, as follows: 2014-dotted curves, 2015-dashed curves, and 2016-solid curves. We observe that all lower records are in 2014, whereas upper records are in 2015 and 2016. Thus, curves showing the lowest speeds are in Autumn, when the temperature starts to slowly decrease. Most of the upper functional records were observed in Spring and Summer, except the last one, observed in September 2016. Summer in Saudi Arabia brings sandstorms driven by Summer South winds. Therefore, it is reasonable to observe these extreme curves.

We can now infer what would be the expected number of record curves for future years. To do this, first, we need to know if the wind speed curves correspond to a functional stationary process, or if there is a possible functional stochastic trend. On the right side of Figure 6, we present the trajectory of the corresponding  $N_j$  process. We apply our RB-functional unit root to the wind speed dataset. The test statistic value is  $T_n = 0.27$ , which is smaller than the corresponding 5% quantile  $q_{0.05} = 0.59$ , even smaller than the 1% quantile  $q_{0.01} = 0.34$ . Thus, we have significant evidence against the stochastic trend, and conclude that the functional wind data do not have a unit root component. Therefore, the number of records expected for daily wind speed curves is with the rate  $\log j$  (Proposition 1). This means that, we expect to get 3 extreme curves, approximately  $(\log(1095))$ , for the following 3 years.

## 6.2 Mortality rates in France

This dataset consists of  $n = 191$  curves of annual mortality rates in France, from 1816 to 2006, for zero to 110-years old individuals. However, we consider only up to 100 years of age in order to avoid highly noisy measurements. Each point of the curve  $X_i(s)$  represents the total

mortality rate, in year  $i$ , at age  $s$ . Our interest is to study the behavior of the rates, over the years, taking into account all ages. By studying records, we analyze whether the new functional records over the years correspond to the natural randomness of the process, or if they indicate a decreasing trend. The data have been analyzed before by [Hyndman and Ullah \(2007\)](#) using a functional approach. They proposed to forecast the age-specific mortality rate by modeling the coefficients obtained by projecting the functional data to the corresponding robust functional principal components. They fitted an ARIMA model to the coefficients, but they did not report the estimated parameters. Evidence of a univariate unit root can be found if we fit the ARIMA model to the first coefficients, for the first eigenfunction. We therefore investigate if there is evidence of a functional unit root. In our analysis, we use the smoothed curves, as described in [Hyndman and Ullah \(2007\)](#).

We exclude the two first curves that are functional records by definition. We find that the years for the corresponding functional records are: 1818, 1819, 1821, 1832, 1845, 1862, 1871, 1897, 1913, 1920, 1923, 1924, 1927, 1930, 1933, 1934, 1937, 1946 – 1948, 1958, 1959, 1961, 1966, 1975, 1977, 1980, 1981, 1984 – 1987, 1992 – 2006. That is 49 functional records in total.

Figure 7 shows the dataset (left) indicated in gray, whereas the functional records are indicated in colors ranging from white to red (heat colors), according to the order in which they appear. On the center of Figure 7, we plot only the record curves. We indicate the upper and lower

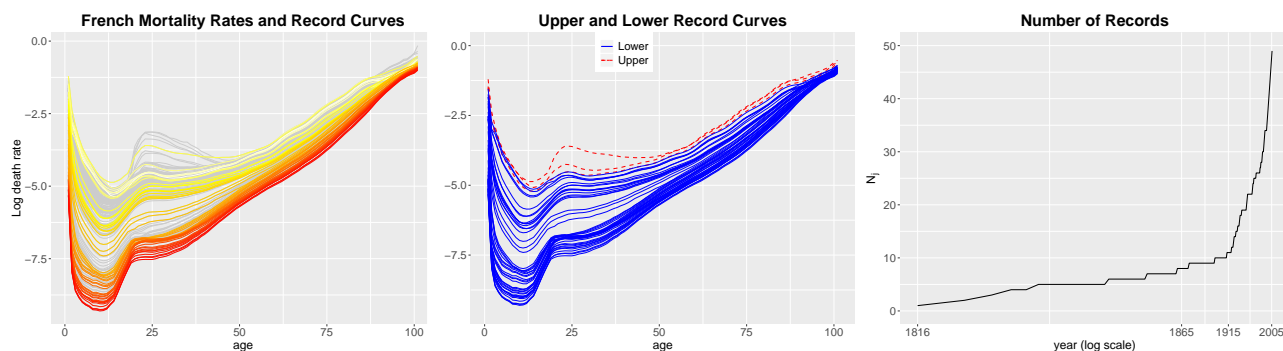


Figure 7: Functional data of log mortality rates in France from 1816 to 2006, for zero to 100 years of age (left), lower records in blue color and upper records in red color (center), and the trajectory of the number of functional records over time (right).

records with different line types: upper functional records with a red dashed curve, and lower functional records with a blue solid curve. We observe only three upper records that correspond to the years 1818, 1832 and 1871. The rest of the records correspond to lower functional records. In particular, we observe that, after the last upper functional records in 1871, a new functional record represents a lower mortality rate for almost all ages. This suggests the presence of a functional trend.

Finally, we apply our RB-functional unit root test to the dataset. On the right side of Figure 7, we show the trajectory of the corresponding  $N_j$  process. The test statistic value is  $T_n = 3.54$ , and the corresponding 5% quantile from the asymptotic distribution under the null hypothesis is  $q_{0.05} = 0.59$ . Therefore, we do not have any evidence against the  $I(1)$  functional process. Thus, to model this dataset, we must consider the existence of both a stochastic trend and a functional deterministic trend. This is consistent with the findings by [Hyndman and Ullah \(2007\)](#) that take into consideration the ARIMA models for the basis coefficients. However, our approach is more general, as we do not consider any specific model.

## 7 Discussion

In this paper, we proposed an extension of the record definition to functional data. We used a depth notion to rank curves and then be able to classify the extreme curves. The definition of a functional record considers jointly the upper and lower records. The extension takes into account the functional characteristics of the data, unlike the pointwise approach. We showed that the counting process corresponding to the number of functional records grows at rate  $\log j$ , for stationary functional time series, and that it grows at rate  $j^{1/2}$ , for nonstationary functional time series. A simulation study showed that the asymptotic distribution of the number of records has a good approximation when the functional data are a functional random walk, even for small sample sizes.

As an application, we proposed a functional unit root test for a general definition of  $I(1)$

functional processes. Using a Monte Carlo simulation study, we showed that the test performance is good for  $I(0)$  and  $I(1)$  functional processes. Our test is robust against structural changes for a moderate sample size. The unit root test based on functional records does not assume any model. In the data application, we found that the definition of functional records provides relevant and consistent information about extremes curves. In addition, it allows us to infer about the underlying process, and the number of expected functional records.

We believe the work presented in this article provides very valuable new information to those interested in extreme value theory for functional data, and offers an interesting alternative method to study extremes for continuous stochastic processes. We to encourage the use of the functional approach to analyze different data applications.

## Appendix: Proofs

### Proof of Proposition 2:

Let  $X_0, X_1, \dots, X_n$  be the functional time series starting at time 0, and  $N_n$  the number of records until time  $n$ . For  $j \geq 2$ , let  $\tilde{R}_j$  be the indicator of  $X_j$  being a functional record but using only three curves: the two most extreme observations until time  $j - 1$ ,  $\{X_0, X_1, \dots, X_{j-1}\}$ , and the new curve  $X_j$ . Specifically, let  $\{\mathbf{Y}_i, i \geq 1\}$  be a bivariate functional process defined as follows:  $\mathbf{Y}_1 = (X_0, X_1)^T$ , and for  $i \geq 2$ ,  $\mathbf{Y}_i = (Y_{i,1}, Y_{i,2})^T$  where  $\{Y_{i,1}, Y_{i,2}\} = \{\text{the two most extreme curves among } \{Y_{i-1,1}, Y_{i-1,2}, X_i\}\}$ . The bivariate process  $\mathbf{Y}_i$  is a constant process until  $X_i$  is not the deepest curve in the three elements set. Then,  $\tilde{R}_j := \mathbb{1}\{X_j \in \{Y_{j,1}, Y_{j,2}\}\}$ .

First, we prove  $\sum_{j=1}^n R_j = \sum_{j=1}^n \tilde{R}_j$ . Clearly  $\tilde{R}_2 = R_2$ . Now, for  $j \geq 3$ . Assume that  $X_j$  is a functional record at time  $j$ , and without loss of generality, assume it is an upper functional record, i.e.,  $\text{fD}(X_j; P) \leq \text{fD}(X_{L^u(j-1)}; P)$ . If there are no ties, i.e.,  $\text{fD}(X_j; P) < \text{fD}(X_{L^u(j-1)}; P)$ , then  $\text{fD}(X_j; P) < \max\{\text{fD}(X_{L^u(j-1)}; P), \text{fD}(X_{L^l(j-1)}; P)\}$  at times  $\{L^u(j-1), L^l(j-1), j\}$ . That is,  $R_j = 1$  implies  $\tilde{R}_j = 1$ . If there are ties, i.e.,  $\text{fD}(X_j; P) = \text{fD}(X_{L^u(j-1)}; P)$ , then we have that

$\text{fD}(X_j; P) \leq \max\{\text{fD}(X_{L^u(j-1)}; P), \text{fD}(X_{L^l(j-1)}; P)\}$ , at times  $\{L^u(j-1), L^l(j-1), j\}$ , in other case there is another curve  $X_{i_0}$ , with  $1 \leq i_0 < j-1$  and  $i_0 \neq L^u(j-1), L^l(j-1)$ , such that  $\text{fD}(X_{i_0}; P) \leq \text{fD}(X_j; P)$ , that is,  $\text{fD}(X_j; P) \leq \text{fD}(X_{i_0}; P) \leq \text{fD}(X_{L^u(j-1)}; P)$ , and as a consequence  $X_{i_0} \sim X_{L^u(j-1)} \sim X_j$ . By Assumption 2 this event as probability zero. Thus,  $R_j = 1$  implies  $\tilde{R}_j = 1$  when ties occur. Therefore  $\sum_{j=1}^n R_j \leq \sum_{j=1}^n \tilde{R}_j$ . Now, assume that  $X_j$  is not a functional record at time  $j$ . Then we have  $\text{fD}(X_j; P) > \text{fD}(X_{L^u(j)}; P)$  and  $\text{fD}(X_j; P) > \text{fD}(X_{L^l(j)}; P)$ , otherwise it would be a functional record. Since  $L^u(j) = L^u(j-1)$  and  $L^l(j) = L^l(j-1)$ , we have that  $\text{fD}(X_j; P) > \max\{\text{fD}(X_{L^u(j-1)}; P), \text{fD}(X_{L^l(j-1)}; P)\}$ , i.e.,  $X_j$  is deeper than  $X_{L^u(j-1)}$  and  $X_{L^l(j-1)}$ . As a consequence  $R_j = 0$  implies  $\tilde{R}_j = 0$ , thus  $\sum_{j=1}^n R_j \geq \sum_{j=1}^n \tilde{R}_j$ . Therefore  $\sum_{j=1}^n R_j = \sum_{j=1}^n \tilde{R}_j$  with probability one.

To prove Proposition 2, we use  $\tilde{R}_j$  instead of  $R_j$ . We consider the bivariate functional time series defined by  $\mathbf{X}_1 = (X_1, X_0)^T, \mathbf{X}_2 = (X_2, X_1)^T, \dots, \mathbf{X}_n = (X_n, X_{n-1})^T$ . We observe that the components of  $\mathbf{X}_1$  are record curves by definition. We denote by  $\boldsymbol{\tau} = \{\tau_1, \dots, \tau_{N_n^u}\}^T$  where  $\tau_1 = 1$ , for  $j = 2, \dots, N_n^u - 1$ ,  $\tau_j$  is the time interval between the upper record  $j$  and  $j+1$ , and  $\tau_{N_n^u} = n - \sum_{j=1}^{N_n^u-1} \tau_j$ .

Let  $\mathbf{Y}_1^u = \mathbf{Y}_1, \dots, \mathbf{Y}_{\tau_1+\tau_2-1}^u = \mathbf{Y}_1, \mathbf{Y}_{\tau_1+\tau_2}^u = \mathbf{Y}_{\tau_1+\tau_2}, \dots, \mathbf{Y}_{\tau_1+\tau_2+\tau_3-1}^u = \mathbf{Y}_{\tau_1+\tau_2}, \mathbf{Y}_{\tau_1+\tau_2+\tau_3}^u = \mathbf{Y}_{\tau_1+\tau_2+\tau_3}, \dots$ . The bivariate process  $\{\mathbf{Y}_j^u\}$  contains upper functional record curves, and it ‘‘jumps’’ when a new upper functional record is observed. We consider the joint distribution  $P(\boldsymbol{\tau}, N_n^u)$  of record times  $\boldsymbol{\tau}$  and number of records  $N_n^u$ .

Since  $X_i$  is a functional random walk, it has the Markov property, and by using the translation invariance with respect to the initial curve, the probability of  $X_i$  being an upper record only depends on  $\mathbf{Y}_{L(N_i^u-1)}^u$  instead of all the past. For a number of curves  $n$ ,

$$P(\boldsymbol{\tau}, N_n^u) = p(\tau_1 | \mathbf{Y}_{\tau_1}^u) p(\tau_2 | \mathbf{Y}_{\tau_1+\tau_2}^u) \cdots p(\tau_{N_n^u-1} | \mathbf{Y}_{L(N_n^u-1)}^u) q(\tau_{N_n^u} | \mathbf{Y}_{L(N_n^u-1)}^u), \quad (8)$$

where  $p(t | \mathbf{Y}) = P(\mathbf{X}_2 \prec \mathbf{Y}, \mathbf{X}_3 \prec \mathbf{Y}, \dots, \mathbf{X}_{t-1} \prec \mathbf{Y}, \mathbf{X}_t \succ \mathbf{Y} | \mathbf{Y})$  and  $q(t | \mathbf{Y}) = P(\mathbf{X}_2 \prec \mathbf{Y}, \mathbf{X}_3 \prec \mathbf{Y}, \dots, \mathbf{X}_t \prec \mathbf{Y} | \mathbf{Y})$ . Because of the translation invariance of  $\{X_i\}$  with respect to the initial

curve,  $p(t|\mathbf{Y})$  and  $q(t|\mathbf{Y})$  do not depend on  $\mathbf{Y}$ . From the way we write the bivariate process, we obtain that  $p(t)$  and  $q(t)$  correspond to a general renewal process. Following [Feller \(1971\)](#), Chap 7, the generating function of  $q(t)$  is

$$\tilde{q}(z) = \sum_{t=0}^{\infty} q(t)z^t = \exp \left\{ \sum_{j \geq 1} \frac{z}{j} P(X_j \leq 0) \right\}.$$

On the other hand, if we consider the generating function of (8) and take the summation over all possible values of components of  $\boldsymbol{\tau}$  and all possible sample sizes  $n$ , we find that, by using  $p(t) = q(t-1) - q(t)$ :

$$\sum_{n=0}^{\infty} P(N_n^u = k)z^n = \{1 - (1-z)\tilde{q}(z)\}^{k-1}\tilde{q}(z), \quad k > 1. \quad (9)$$

Since the distribution of the functional white noise  $\varepsilon_0$  is assumed to be symmetric, then  $P(X_i \leq 0) = 1/2$ . Therefore  $\tilde{q}(z) = \frac{1}{\sqrt{1-z}}$ . Using this result in (9) and taking the limit as  $n \rightarrow \infty$ , we obtain that  $N_n^u/\sqrt{n} \xrightarrow{d} G_1$ , where  $G_1$  has density  $g_1(x) = \frac{1}{\sqrt{\pi}} \exp(-x^2/4)$  for  $x \geq 0$ . □

**Proof of Proposition 3:** Let  $\{X_i\}$  be an  $I(1)$  functional process, then  $X_i$  can be written as  $X_i = Z_0(s) + \Psi \left( \sum_{j=1}^i \varepsilon_j \right) (s) + \nu_i(s)$ . Let  $C_{\nu_i}$  be the covariance operator of  $\nu_i$ , and we observe that the covariance operator of  $\Psi \left( \sum_{j=1}^n \varepsilon_j \right)$  is  $n\Psi C_{\varepsilon_0} \Psi^*$ , where  $C_{\varepsilon_0}$  is the covariance operator of  $\varepsilon_0$ . Then, when  $n$  is large, the variance of  $X_n$  is driven by the variance of the process  $\Psi \left( \sum_{j=1}^n \varepsilon_j \right)$ . Without loss of generality, we assume that there is no stationary component, that is,  $\nu_i = 0$ .

Now, let  $v \in \text{ran } \Psi$ , then  $\langle X_i, v \rangle = \langle Z_0, v \rangle + \langle \Psi \left( \sum_{j=1}^i \varepsilon_j \right), v \rangle = Z_0^v + \sum_{j=1}^i \langle \varepsilon_j, \Psi^* v \rangle$ , where  $Z_0^v$  is a scalar. Also,  $\langle \varepsilon_j, \Psi^* v \rangle$  is an independent random variables with non-degenerate distribution, since  $\text{ran } \Psi^* \subseteq (\ker \Psi)^\perp$  and  $\Psi^* v \neq 0$ . Therefore,  $\{\langle X_i, v \rangle\}$  is a random walk for all  $v \in \text{ran } \Psi$ . As a consequence, the number of records of  $\{X_i\}$  on  $\text{ran } \Psi$  has the same asymptotic distribution as a functional random walk. Finally, the functional depth is not computed only on the subspace  $\ker \Psi$  with probability one because of the nondegeneracy of functional depth. In addition,  $X_n$  is driven by the variance of the process  $\Psi \left( \sum_{j=1}^n \varepsilon_j \right)$ . These facts allow us to conclude that the



number of records on  $\{X_i\}$  has the same asymptotic distribution as a functional random walk on the whole space  $\mathcal{H}$ . □

**Proof of Corollary 1:**

Similarly to the counting process  $N_n^u$ , we have that  $N_n^l/\sqrt{n} \xrightarrow{d} G_1$ , where  $N_n^l$  is the corresponding counting process for the lower functional records. For renewal processes, we know that the asymptotic joint distribution of  $(N_n^u/\sqrt{n}, N_n^l/\sqrt{n})$  is equal to the joint distribution of  $(|W(1)|, l(0, 1))$ , where  $W(s)$  is the Brownian motion and  $l(0, 1)$  is the local time of the Brownian motion at zero, evaluated at one. On the other hand  $(|W(t)|, l(0, t))$  and  $(\max_{0 \leq s \leq t} W(s) - W(t), \max_{0 \leq s \leq t} W(s))$  have the same joint density  $f_0(x, y)$ . Using that the joint density function of  $(\max_{0 \leq s \leq t} W(s), W(t))$  is  $f(m, w) = \sqrt{\frac{2}{\pi t^{3/2}}}(2m - w) \exp\{-(2m - w)^2/2t\}$ , we obtain that  $f_0(x, y) = \sqrt{\frac{2}{\pi t^{3/2}}}(x + y) \exp\{-(x + y)^2/2t\}$ . Using a bivariate transformation of the random variables, we obtain that the asymptotic distribution of  $(N_n^u + N_n^l)/\sqrt{n}$  has density  $g_2(x) = \sqrt{\frac{2}{\pi}} x^2 \exp(-x^2/2)$ ,  $x \geq 0$ . □

## References

Ahsanullah, M. and V. B. Nevzorov (2015). *Records via Probability Theory*, Volume 6 of *Atlantis Studies in Probability and Statistics*. Atlantis Press, Paris.

Aparicio, F., A. Escibano, and A. E. Sipols (2006). Range unit-root (RUR) tests: robust against nonlinearities, error distributions, structural breaks and outliers. *Journal of Time Series Analysis* 27(4), 545–576.

Aue, A., D. D. Norinho, and S. Hörmann (2015). On the prediction of stationary functional time series. *Journal of the American Statistical Association* 110(509), 378–392.

Ballerini, R. and S. I. Resnick (1987). Records in the presence of a linear trend. *Advances in Applied Probability* 19(4), 801–828.

Beare, B. K., J. Seo, and W.-K. Seo (2017). Cointegrated linear processes in Hilbert space. *Journal of Time Series Analysis* 38(6), 1010–1027.

Bosq, D. (2000). *Linear Processes in Function Spaces*, Volume 149 of *Lecture Notes in Statistics*. Springer-Verlag, New York. Theory and applications.

Burridge, P. and E. Guerre (1996). The limit distribution of level crossings of a random walk, and a simple unit root test. *Econometric Theory* 12(4), 705–723.

- Chakraborty, A. and P. Chaudhuri (2014a). On data depth in infinite dimensional spaces. *Annals of the Institute of Statistical Mathematics* 66(2), 303–324.
- Chakraborty, A. and P. Chaudhuri (2014b). The spatial distribution in infinite dimensional spaces and related quantiles and depths. *The Annals of Statistics* 42(3), 1203–1231.
- Dickey, D. A. and W. A. Fuller (1979). Distribution of the estimators for autoregressive time series with a unit root. *Journal of the American Statistical Association* 74(366), 427–431.
- Dombry, C. and M. Zott (2018). Multivariate records and hitting scenarios. *Extremes* 21(2), 343–361.
- Donoho, D. L. (1982). Breakdown properties of multivariate location estimators. Ph.D. qualifying paper, Harvard University.
- Dufour, J.-M. (2006). Monte Carlo tests with nuisance parameters: a general approach to finite-sample inference and nonstandard asymptotics. *Journal of Econometrics* 133(2), 443–477.
- Falk, M., A. Khorrami Chokami, and S. A. Padoan (2018). On multivariate records from random vectors with independent components. *Journal of Applied Probability* 55(1), 43–53.
- Feller, W. (1971). *An Introduction to Probability Theory and its Applications. Vol. II.* Second edition. John Wiley & Sons, Inc., New York-London-Sydney.
- Fraiman, R., A. Justel, R. Liu, and P. Llop (2014). Detecting trends in time series of functional data: a study of Antarctic climate change. *The Canadian Journal of Statistics. La Revue Canadienne de Statistique* 42(4), 597–609.
- Fraiman, R. and G. Muniz (2001). Trimmed means for functional data. *TEST* 10(2), 419–440.
- Gijbels, I. and S. Nagy (2017). On a general definition of depth for functional data. *Statistical Science* 32(4), 630–639.
- Gnedin, A. V. (1998). Records from a multivariate normal sample. *Statistics & Probability Letters* 39(1), 11–15.
- Goldie, C. M. and S. Resnick (1989). Records in a partially ordered set. *The Annals of Probability* 17(2), 678–699.
- Goldie, C. M. and S. I. Resnick (1995). Many multivariate records. *Stochastic Processes and their Applications* 59(2), 185–216.
- Hörmann, S. and P. Kokoszka (2010). Weakly dependent functional data. *The Annals of Statistics* 38(3), 1845–1884.
- Horváth, L., M. Hušková, and P. Kokoszka (2010). Testing the stability of the functional autoregressive process. *Journal of Multivariate Analysis* 101(2), 352–367.
- Huang, H. and Y. Sun (2019). A decomposition of total variation depth for understanding functional outliers. *Technometrics*. To appear.

- Hyndman, R. J. and M. S. Ullah (2007). Robust forecasting of mortality and fertility rates: a functional data approach. *Computational Statistics & Data Analysis* 51(10), 4942–4956.
- Kokoszka, P. and M. Reimherr (2013). Determining the order of the functional autoregressive model. *Journal of Time Series Analysis* 34(1), 116–129.
- Lindgren, G. and H. Rootzén (1987). Extreme values: theory and technical applications. *Scandinavian Journal of Statistics* 14(4), 241–279.
- López-Pintado, S. and J. Romo (2009). On the concept of depth for functional data. *Journal of the American Statistical Association* 104(486), 718–734.
- López-Pintado, S. and J. Romo (2011). A half-region depth for functional data. *Computational Statistics & Data Analysis* 55(4), 1679–1695.
- Martínez-Hernández, I., M. G. Genton, and G. González-Farías (2019). Robust depth-based estimation of the functional autoregressive model. *Computational Statistics & Data Analysis* 131, 66–79.
- Muriel, N. (2015). The functional AR(1) process with a unit root. *arXiv:1512.01844*.
- Narisetty, N. N. and V. N. Nair (2016). Extremal depth for functional data and applications. *Journal of the American Statistical Association* 111(516), 1705–1714.
- Nieto-Reyes, A. and H. Battey (2016). A topologically valid definition of depth for functional data. *Statistical Science* 31(1), 61–79.
- Ramsay, J. O. and B. W. Silverman (2005). *Functional Data Analysis* (Second ed.). Springer Series in Statistics. Springer, New York.
- Rousseeuw, P. J. and M. Hubert (1999). Regression depth. *Journal of the American Statistical Association* 94(446), 388–402.
- Sguera, C., P. Galeano, and R. Lillo (2014). Spatial depth-based classification for functional data. *TEST* 23(4), 725–750.
- Sparre Andersen, E. (1954). On the fluctuations of sums of random variables. II. *Mathematica Scandinavica* 2, 195–223.
- Stahel, W. (1981). Breakdown of covariance estimators. Research report 31, Fachgruppe für Statistik, E.T.H. Zürich, Switzerland.
- Sun, Y. and M. G. Genton (2011). Functional boxplots. *Journal of Computational and Graphical Statistics* 20(2), 316–334.
- Wergen, G., S. N. Majumdar, and G. Schehr (2012). Record statistics for multiple random walks. *Physical Review E* 86(1).
- Zuo, Y. (2003). Projection-based depth functions and associated medians. *The Annals of Statistics* 31(5), 1460–1490.